

Making 802.11 DCF Near-Optimal: Design, Implementation, and Evaluation

Jinsung Lee, Hojin Lee, Yung Yi, *Member, IEEE*, Song Chong, *Member, IEEE*, Edward W. Knightly, *Fellow, IEEE*, and Mung Chiang, *Fellow, IEEE*

Abstract—This paper proposes a new protocol called *Optimal DCF* (O-DCF). O-DCF modifies the rule of adapting CSMA parameters, such as backoff time and transmission length, based on a function of the demand–supply differential of link capacity captured by the local queue length. O-DCF is fully compatible with 802.11 hardware, so that it can be easily implemented only with a simple device driver update. O-DCF is inspired by the recent analytical studies proven to be optimal under assumptions, which often generates a big gap between theory and practice. O-DCF effectively bridges such a gap, which is implemented in off-the-shelf 802.11 chipset. Through extensive simulations and real experiments with a 16-node wireless network testbed, we evaluate the performance of O-DCF and show that it achieves near-optimality in terms of throughput and fairness and outperforms other competitive ones, such as 802.11 DCF, optimal CSMA, and DiffQ for various scenarios. Also, we consider the coexistence of O-DCF and 802.11 DCF and show that O-DCF fairly shares the medium with 802.11 via its parameter control.

Index Terms—802.11 DCF, experiment, optimal CSMA, testbed implementation.

I. INTRODUCTION

EXTENSIVE research documents inefficiency and unfairness of the standard 802.11 DCF and suggests ways to improve it. Some proposals take a clean-slate approach to redesign CSMA. For some of them, optimality in performance can sometimes be proved under idealized assumptions such as no collision or perfect synchronization. Other solutions are constrained to operate over legacy 802.11 hardware with only a

device driver update, but their performance improvements are often marginal. Among prior methods to improve 802.11 DCF is the seemingly conflicting pair of random access philosophies: In the face of collisions, should transmitters become more aggressive given that the supply of service rate may become lower than the demand (as in the recently developed theory of Optimal CSMA (oCSMA), e.g., [1]–[5])? Or should they become less aggressive given that collisions signal a contentious RF environment (as in a typical exponential backoff in 802.11 DCF)?

In this paper, we propose a new protocol, called *Optimal DCF* (O-DCF),¹ showing that the two approaches are in fact complementary, where the best combination depends on the logical contention topology, but can be learned without knowing the topology. O-DCF is inspired on the ideas of CSMA adaptation developed by different analytical optimization work [1]–[5], but it is designed to: 1) be fully compatible with off-the-shelf 802.11 chipsets; and 2) achieve high performance in practice by tackling practical issues encountered in actual deployment, which are largely ignored in theory, yet have high impact on actual performance.

In O-DCF, a product of access probability, which is determined by contention window (CW) size, and transmission length is set to be proportional to the supply–demand differential for long-term throughput fairness. Toward the goal of achieving high performance in practice, a good combination of access probability and transmission length is taken, where such a good access probability is “searched” by Binary Exponential Backoff (BEB) in a fully distributed manner to adapt to the contention levels in the neighborhood, and then transmission length is suitably selected for long-term throughput fairness. Thus, BEB is exploited not just to conservatively respond to temporal collisions, as in standard 802.11, but also to be adapted to appropriate access aggressiveness for high long-term fairness and throughput by being coupled with the transmission length.

We first summarize three key design ideas of O-DCF.

- D1) Link access aggressiveness is controlled by both CW size and transmission length, based on per-neighbor local queue length at MAC layer, where the queue length quantifies supply–demand differential. Links with bigger differential (i.e., more queue buildup) are prioritized in media access by decreasing CW size and/or increasing transmission length.
- D2) The CW size and transmission length are adapted in a fully distributed manner, depending on network

Manuscript received March 24, 2014; revised January 15, 2015; accepted April 09, 2015; approved by IEEE/ACM TRANSACTIONS ON NETWORKING Editor E. Ekici. Date of publication June 01, 2015; date of current version June 14, 2016. This work was supported by the Center for Integrated Smart Sensors under Grant CISS-2012M3A6A6054195 funded by the Ministry of Science, ICT & Future Planning as Global Frontier Project, the National Research Foundation of Korea (NRF) under Grant NRF-2013R1A2A2A01067633 funded by the Korea Government (MSP), Cisco Systems, Intel, the Keck Foundation, and the NSF under Grants CNS-1444056, CNS-1126478, CNS-1012831, CNS-1318607, and CNS-1456847.

J. Lee is with the DMC R&D Center of Samsung Electronics, Suwon 443-742, Korea (e-mail: js81.lee@samsung.com).

H. Lee is with the Software R&D Center of Samsung Electronics, Suwon 443-742, Korea.

Y. Yi and S. Chong are with the Department of Electrical Engineering, Korea Advanced Institute of Science and Technology (KAIST), Daejeon 305-338, Korea.

E. W. Knightly is with the Department of Electrical and Computer Engineering, Rice University, Houston, TX 77005 USA.

M. Chiang is with the Department of Electrical Engineering, Princeton University, Princeton, NJ 08544 USA.

Color versions of one or more of the figures in this paper are available online at <http://ieeexplore.ieee.org>.

Digital Object Identifier 10.1109/TNET.2015.2432053

¹We just use the word “optimal” because our protocol is inspired in part by the recent CSMA theory, called optimal CSMA.

topology affecting contention patterns in the neighborhood. Each link first chooses the initial CW size as a decreasing function of the local queue length and increases the CW size against collisions (i.e., BEB). Then, transmission length is decided by a “smart” combination of the resulting CW size (at which transmission succeeds) and the local backlog.

- D3) When wireless channels are heterogeneous across links, e.g., a 2-Mb/s link and another 6-Mb/s link, the link capacity information is reflected in controlling access aggressiveness by scaling the queue length proportionally to the link capacity. This adaptive control based on link capacity ensures better fairness and higher throughput since links with better channel condition are scheduled more than those with poor channel condition.

In D2, for the case when nodes can sense each other and contends symmetrically, the CW size is appropriately chosen to be a reasonably low value to reduce collisions, and then the transmission length is chosen to be a function of queue length. For the topology with asymmetric contentions, e.g., flow-in-the-middle (FIM),² where inner and outer links have different contention degrees, the CW size of a link that experiences more contention is adjusted to be smaller than those of other links with less contention, so that it can get enough transmission chances and thus fairness is ensured. We show that this selective control of CSMA parameters works well even in challenging topologies in which 802.11 DCF yields severe performance degradation, such as hidden terminal (HT), information asymmetry (IA), FIM, and packet capture.

The key design ideas mentioned above are implemented through the following protocol mechanisms.

- P1) Each transmitter maintains two queues for each neighbor, referred to as Control Queue (CQ) and Media Access Queue (MAQ). CQ buffers the packets from the upper-layer that are to be dequeued into MAQ. The length of MAQ refers to the local queue length in D2, determining access aggressiveness by adjusting CW size and transmission length. The dequeue rate from CQ to MAQ is controlled through the MAQ length to ensure various, tunable fairness criteria, and high throughput.
- P2) Once the initial CW size is chosen as a function of the length of MAQ, BEB “searches” for the CW size at which transmission becomes successful in a fully distributed manner. This successful CW size is used to choose the transmission length as described in D2.
- P3) We adapt transmission length based on time rather than bytes to achieve time fairness even under heterogeneous channels. To that end, we exploit instantaneous link information from the rate-adaptation module in the 802.11 driver to determine the proper number of bytes to send, according to modulation and coding rate in use.

All of the above mechanisms can be implemented using unmodified 802.11 chips, as we have done in evaluating O-DCF over a 16-node wireless testbed. In particular, the mechanisms satisfy the following constraints of operation over 802.11.

- C1) *Interface queue (IQ)*. 802.11 hardware uses a single queue called IQ, which is shared by all local flows for

storing packets ready for actual transmission to the media, and for neighbor-specific packet control necessitates additional queues such as CQ and MAQ on top of the IQ.

- C2) *CW granularity*. CW values are allowed by only some powers of two due to chipset-level complexity reduction, and thus we can only choose the value from the set $\{2^n - 1, n = 1, \dots, 10\}$.
- C3) *Maximum aggregate frame size*. The transmission length is bounded by some value that depends on the 802.11 chipset. For instance, it is determined by the minimum of maximum allowable time and maximum aggregation size, e.g., 64 kB in 802.11n [6].

To evaluate the performance of O-DCF, we have implemented O-DCF on a 16-node wireless testbed as well as a simulator for large-scale scenarios that are difficult to be configured in the real testbed. By comparing O-DCF to 802.11 DCF, two versions of oCSMA, and DiffQ [7], we observe that in presence of conditions that are known to be critical to other CSMA protocols, O-DCF achieves near-optimal throughput, fairly distributed among flows, with up to 87.1% fairness gain over 802.11 DCF.

II. RELATED WORK

Numerous papers have reported the performance problems of 802.11 DCF and proposed many solutions to them. To name just a few, 802.11 DCF has severe performance degradation and throughput disparities among contending flows in the topologies such as Hidden-terminal (HT), information asymmetry (IA), flow-in-the-middle (FIM), and packet capture [8]–[11] and heterogeneous link capacities [12]. We classify the solution proposals into the efforts at MAC and/or PHY. Some papers proposed new access methods such as dynamic adjustment of CW under 802.11 DCF, e.g., [13] and [14], and there exist the implementation researches along this line, e.g., [15] and [16]. Other work presented efficient aggregation schemes and their real implementations for throughput improvement, e.g., [17] and [18]. Note that most implementations mentioned above individually focused on some specific topologies such as fully connected (FC) case, and do not explicitly consider problematic ones such as HT, IA, and FIM. With the aid of PHY-layer, there are totally novel approaches, e.g., [19] and [20]. This kind of work exploits more information from PHY layer and/or applies new PHY technologies other than CSMA. In O-DCF, we extend MAC-level operation *by controlling the CW size as well as the transmission length based on the demand–supply differential*. The PHY-layer-based approach is somewhat orthogonal to our approach, which even can be integrated with O-DCF for further performance improvement.

Recently, analytical studies proved that, under certain assumptions, queue-length-based scheduling via CSMA can achieve maximum throughput without message passing, e.g., [1]–[3], which is referred to as oCSMA in this paper. Furthermore, multiple theoretical papers presented solutions based on the similar mathematical framework, each of them focusing on different aspects of the protocol operation, e.g., [4], [5], [21], and [22] (see [23] for a survey). Our work is in part motivated by oCSMA theory, but as reported in [24], [25], and our evaluation, there still exist many gaps between oCSMA

²Throughout this paper, we use “flow” and “link” interchangeably.

theory and 802.11 practice. There exists work that bridges the gaps between theory on queue-based MAC (not necessarily CSMA) and practice by reflecting queue length over 802.11 [7], [26], [27]. In [7], the authors implemented a heuristic differential backlog algorithm (DiffQ) over 802.11e. EZ-Flow was proposed to solve instability due to large queue build-ups in 802.11 mesh networks [26]. Very recently, the authors in [27] implemented a backpressure scheduling based on TDMA MAC, which operates in a centralized way. In contrast with the aforementioned work, we present the first asynchronous CSMA-based protocol, motivated by optimal CSMA theory and designed to work on top of the legacy 802.11 hardware, that can attain high performance even in several adverse scenarios.

III. WHY DOESN'T OCSMA WORK

A. Optimal CSMA Algorithm

oCSMA is a variant of CSMA that has a specific rule of setting the backoff³ and holding time. Algorithm 1 summarizes how oCSMA works. The key to achieve optimality in throughput and fairness lies in the fact that a link l running oCSMA determines its access probability p_l , and holding time μ_l , *adaptively* to the link queue length q_l . Given that time is divided into frames,⁴ let $\text{CSMA}(p, \mu)$ be the CSMA having a random backoff time with mean $1/p$ and a random transmission duration with mean μ . The queue lengths are updated as in (1), where $A_l[t]$ is the amount of incoming packets (to the MAC layer) at frame t , and $S_l[t]$ is the amount of served packets at frame t over link l , and b is a step-size at frame t . We define the *access aggressiveness* of link l as the product of p_l and μ_l , and hence, it represents the aggressiveness of link l 's transmission attempts. As in (2), the access aggressiveness is equal to $\exp(q_l)$, where q_l is the queue length scaled by the positive step-size b .

Algorithm 1: Optimal CSMA

- 1: During frame t , the transmitter of link l runs $\text{CSMA}(p_l[t], \mu_l[t])$, and records the amount $S_l[t]$ of service received during this frame;
- 2: At the end of frame t , the queue of link l is updated according to

$$q_l[t+1] = [q_l[t] + b(A_l[t] - S_l[t])]_{q_{\min}}^{q_{\max}} \quad (1)$$

- 3: Channel access probability p_l and holding time μ_l are updated such that

$$p_l[t+1] \cdot \mu_l[t+1] = \exp(q_l[t+1]). \quad (2)$$

B. Limitation of Optimal CSMA in Practice

The effectiveness of oCSMA and its underlying MAC design approach is proven under critical assumptions. For example, oCSMA does not assume any packet collisions or imperfect carrier sensing by either topological factors or channel asymme-

³The backoff counter is chosen randomly from the interval $[0, CW]$, thus the access probability in a min-slot can be computed by $p_l = 2/CW_l + 1$, as adopted in literature, e.g., [13] and [14].

⁴The frame does not have to be synchronized, and even its duration can be varying, because it just defines the time instants when the states change.

tries. In this section, we analyze why oCSMA can be seriously hurt in practice.

1) *Packet Collisions*: In CSMA, transmitters with backlogged data sense the channel before actual transmission for some random period, referred to as the backoff time. Even if the whole transmitters are in the sensing range of each other, they always have a probability of packet collisions, which is equal to a chance that they select the same backoff time. In response to packet collisions, 802.11 DCF leads to an increase in the CW size at the transmitters via BEB mechanism. However, oCSMA performs in the opposite way as packet collisions imply a reduction on the service rate at the receivers followed by queue growth and increased access aggressiveness.

Our simulation results in Fig. 6(a) of Section VI support these arguments. We control contention level by varying the number of flows. As the contention level grows, there is a big difference between 802.11 and CW adaptation (for now, we consider CW adaptation as our basic oCSMA, and will explain the details in Section VI-A). In fully connected topology with 12 flows (i.e., extreme contention level), the throughput of oCSMA flows is approximately less than a third of that of 802.11.

We find that oCSMA's philosophy of increasing contention aggressiveness with flow queue length is inefficient in fully connected scenarios with high collision probability.

2) *Sensing Imperfection*: It is well known that the presence of hidden terminals can make sensing fail, thus increasing the probability of packet collisions. In addition, if either there is a gap in signal strength from hidden terminals or receivers are also hidden to each other, the symmetry can be broken and one flow interferes with another, but not vice versa. For such circumstances, we consider some representative topologies such as HT, HT with capture, and IA (see Fig. 5 in Section V).

In these scenarios, 802.11 DCF triggers BEB due to packet collisions and lowers the attempt rate to timescales over the packet transmission time, which reduces the collision probability to moderate levels and improves throughput. Also, via RTS/CTS mechanism, it can move collisions from long data packets to shorter control packets. However, this is not always valid, as shown in Fig. 9(b) and (c) in Section VI.

On the other hand, oCSMA operates insufficiently in the presence of hidden terminals because it tries to increase access aggressiveness with flow queue length under packet collisions. In HT, a symmetric increase of access aggressiveness at both flows exacerbates the situation by making a self-sustaining loop of collision \rightarrow queue buildup \rightarrow high aggressiveness \rightarrow small backoff time \rightarrow further collision and repeats. In HT with asymmetry and IA, either flow with weak signals or disadvantageous flow only falls into such a loop, thus amplifying throughput disparities.

We find that oCSMA's self-sustaining loop is not desirable especially in the topologies formed by sensing imperfection.

3) *Channel Errors*: In 802.11 DCF, BEB doubles the CW size upon each transmission failure. Under high contention, this rule reduces the probability of packet collisions. However, in the presence of lossy channel, it can penalize traffic flows with higher loss rates, delaying their access to the channel.

In contrast, over packet losses, oCSMA increases the flow queue length as mentioned before. In turn, this is interpreted as a signal to increase the channel contention aggressiveness at the transmitter. Thus, oCSMA assigns higher access priorities

to lower-quality links. Although this may increase the service rate of disadvantaged flows, it is likely to reduce network efficiency compared to opportunistic scheduling that takes advantage of channel fluctuation. The above analysis is confirmed by experiments, as shown in Fig. 10 in Section VI. This experiment was performed for the case where all links have different PHY rates. However, we also observed that oCSMA shows equal throughput distribution even in the case where all links use the same PHY rate with different packet error rates (e.g., due to LOS/NLOS channels).

We find that oCSMA targets an even distribution of flow throughput, as opposed to a proportional-fair distribution where each link attains a throughput proportional to its capacity. In Section IV, we present our new protocol called O-DCF, which addresses the aforementioned problems at a time.

IV. HOW DOES O-DCF WORK?

We start by listing four key elements in O-DCF.

- 1) *Section IV-A.* Each transmitter is equipped with two queues for each neighbor, CQ and MAQ. CQ is a buffer to store the packets from the upper layer, and its dequeue rate into MAQ is controlled by a certain rule in strict relation to proportional fairness.
- 2) *Section IV-B.* The size of MAQ, which quantifies the differential between demand and supply, is used to control the link access aggressiveness by adjusting CW size and transmission length. First, the initial CW size is determined by a sigmoid function of the size of MAQ, and then BEB is applied for collisions. Thus, the link is prioritized when the demand-supply differential becomes large.
- 3) *Section IV-C.* The transmission length of each link is calculated right after the success CW size, i.e., the CW size at which transmission succeeds, is obtained (with MAQ size as explained earlier). Typically, the success CW size is hard to know from the device driver in real time (due to access overhead), thus we employ a method of estimating the success CW size.
- 4) *Section IV-D.* Channel heterogeneity is reflected by scaling the MAQ size by the link capacity. This gives more priority to the links with better channel conditions in media access, ensuring more efficient rate allocation in terms of time-based fairness.

A. Balancing Supply–Demand Differential

In 802.11 DCF, the packets from the upper layer are enqueued to IQ at the 802.11 chip for media access. In O-DCF, we additionally maintain two per-neighbor queues (CQ and MAQ) over IQ, to balance the link's supply and demand through fair media access, as shown in Fig. 1. Denote by $Q_l^C(t)$ and $Q_l^M(t)$ the lengths of CQ and MAQ for each link l at time t . We further maintain a variable $q_l^M(t)$, which is simply the scaled version of $Q_l^M(t)$, i.e., $q_l^M(t) = bQ_l^M(t)$, where b is some small value.⁵ Finally, the value of $Q_l^M(t)$ is crucial in O-DCF in that both the dequeue rate from CQ to MAQ and the aggressiveness of media access tightly rely on $Q_l^M(t)$.

First, we control the dequeue rate from CQ to MAQ (when CQ is nonempty), such that it is inversely proportional to $q_l^M(t)$,

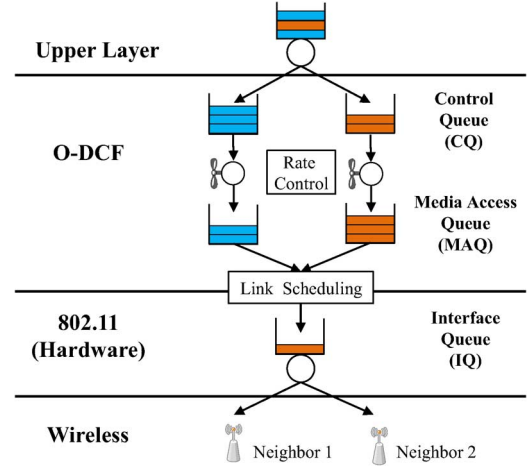


Fig. 1. Queue structure of O-DCF.

by $V/q_l^M(t)$,⁶ where V is some constant controlling the sensitivity of the dequeue rate to MAQ. Second, in terms of aggressiveness in media access, an initial CW size and transmission length, which determine the dequeue rate of MAQ, is set as a function of $q_l^M(t)$ (see Sections IV-B and IV-C for details). Then, whenever a new arrival from CQ or a service (i.e., packet transmission) from successful media access occurs, $Q_l^M(t)$ is updated by

$$Q_l^M(t + \delta t) = [Q_l^M(t) + (\text{arrival from CQ} - \text{service from MAQ})]_{Q_{\min}}^{Q_{\max}} \quad (3)$$

where δt is the elapsed time of the next arrival or service event after t . The service from MAQ occurs when the head-of-line (HOL) packet of MAQ is moved into IQ. For multiple neighbors, the largest MAQ is served first; if the chosen transmission length exceeds a single packet size, multiple packets from the same MAQ are scheduled in succession. Q_{\max} is the physical buffer limit of MAQ, but Q_{\min} is set as a small positive value to prevent impractically high injection rate from CQ to MAQ, when $Q_l^M(t)$ (and thus $q_l^M(t)$) approaches zero.

B. Initial CW with BEB

When a link l is scheduled at time t , its initial CW size ($CW_l(t)$) and the number of bytes to transmit ($\mu(t)$) are set adaptively as a function of the length of MAQ. First, $\mu(t)$ -byte transmission over l is assigned with the following CW size:

$$CW_l(t) = \frac{2(\exp(q_l^M(t)) + C)}{\exp(q_l^M(t))} - 1 \quad (4)$$

where C is some constant whose suitable value will be discussed in Section V-B. We want to use $CW_l(t)$ as the minimum CW (CW_{\min}) in 802.11 DCF. However, since the 802.11 hardware only allows CW values as powers of two, we use one of possible values closest to (4) as CW_{\min} . Then, the media access is attempted after the time (in mini-slots) randomly chosen from the interval $[0, CW_{\min}]$. Intuitively, we assign higher aggressiveness in media access for larger MAQ size, remarking that

⁵The value b is referred to as a step-size in theory, which is used to slow down the variation of queue lengths, as well as to have feasible CW sizes in the aggressiveness update; see Section VII.

⁶This form of injection pattern is for achieving proportional fairness. However, as will be explained in Section V-A, this can be changed towards other fairness criterion.

(4) is decreasing with $q_l^M(t)$. Whenever collision happens, this CW value increases exponentially by BEB. In Section V-B, we will explain that BEB is not just a component often constrained by some legacy 802.11 hardware,⁷ but is an important component to choose an appropriate access aggressiveness and reduce collisions inside our design rationale in a distributed manner.

It is often convenient to interpret CW_l with its corresponding access probability p_l using the relation $p_l = 2/(CW_l + 1)$ [13], [14], where the initial CW_l selection in (4) is regarded as the following *sigmoid* function:

$$p_l(t) = \frac{\exp(q_l^M(t))}{\exp(q_l^M(t)) + C}. \quad (5)$$

We delay our discussion on why and how this sigmoidal type function helps and what choice of C is appropriate to Section V-B.

C. Transmission Length Selection

Our method for the adaptation of the transmission length $\mu_l(t)$ upon channel access by link l is to set $\mu_l(t)$ as a function of the success access probability (equivalently, the success CW size) and the size of MAQ (i.e., $Q_l^M(t)$). Again, by the success CW size, we mean that the transmission becomes successful at that CW size, which is often larger than the initial CW size due to BEB. The rationale to search for the success CW size lies in the fact that it is the actual value used in media access for successful transmission. However, it usually requires quite high overhead for the device driver to read such a success CW size in real time, which may result in delaying packet scheduling. Thus, we estimate it based on the equation [29] that describes the connection between the initial CW (CW_l), collision ratio (p_c), and the success access probability after BEB (denoted by \tilde{p}_l), given by

$$\tilde{p}_l = \frac{2q(1 - p_c^{m+1})}{(CW_l + 1)(1 - (2p_c)^{m+1})(1 - p_c) + q(1 - p_c^{m+1})} \quad (6)$$

where $q = 1 - 2p_c$ and m is the maximum retransmission limit. The collision ratio p_c can be computed for arbitrary topologies [9], only if nodes have the complete knowledge of topology via message passing. To avoid such message passing, we measure the packet collisions by counting the number of unacked packets and normalizing them. Using $\tilde{p}_l(t)$, in O-DCF, the transmission length (in mini-slots) is chosen by

$$\mu_l(t) = \min \left(\frac{\exp(q_l^M(t))}{\tilde{p}_l(t)}, \bar{\mu} \right) \quad (7)$$

where $\bar{\mu}$ is the maximum transmission length (e.g., 64 kB and 10 ms as mentioned earlier, in order to ensure the minimum short-term fairness and prevent channel monopolization by some node). Then, we convert the transmission length in the unit of mini-slots of the 802.11 chipset into that in bytes to compute the number of packets for aggregate transmission by μ_l (bytes) = μ_l (slots) $\times c_l$ (Mb/s) $\times t_{\text{slot}}$ ($\mu\text{s}/\text{slot}$). When

⁷In literature, e.g., [28], it is known that BEB can be disabled by using TXQ descriptor in the device driver, which, however, does not work in our chipset, confirmed via our kernel level measurement.

only a part of μ_l bytes is transmitted due to packetization, we maintain a *deficit counter* to store the remaining bytes of the transmission length that will be used in the next transmission.

D. Channel Heterogeneity and Imperfect Sensing

In practice, wireless channels are heterogeneous across users as well as often time-varying. In such environments, most 802.11 hardware exploits multirate capability of the PHY layer to adapt their rate, e.g., SampleRate [30]. However, it is known that 802.11 DCF is incapable of utilizing this opportunistic feature, leading to the waste of resource called *performance anomaly* [12]. In other words, 802.11 DCF provides equal chances to the links (on average), in which case the low-rate links would occupy more time than the high-rate ones, so that the performance degrades. To provide fairness focusing on time shares instead of rate shares, namely *time-fairness* [31], we slightly modify our rules in selecting the initial access probability as well as the transmission length by replacing $\exp(q_l^M(t))$ with $\exp(c_l(t)q_l^M(t))$ in (4) and (7), where $c_l(t)$ is (relative) link capacity of link l at time t , as theoretically verified by [32]. For imperfect sensing cases such as HT and IA scenarios, we also propose to use a virtual carrier sensing via RTS/CTS signaling, as suggested in literature. In O-DCF, unlike in the standard 802.11a/b/g, RTS/CTS signaling is conducted only for the first packet within the transmission length.

V. WHY DOES O-DCF WORK?

A. Transferring From Theory to Practice

O-DCF is in part motivated by the recent research on queue-based MAC scheduling in theory community, see, e.g., a survey [33] and, in particular, so-called oCSMA [1]–[5]. oCSMA is characterized as a variant of CSMA that has a specific rule of setting backoff time and transmission length. The papers in literature are slightly different in terms of the models and conditions, e.g., discrete/continuous, synchronous/asynchronous, or saturated/unsaturated traffic. However, the key idea is largely shared; the queue maintains the demand–supply differential, and the access aggressiveness is controlled by the queue length, which, in turn, depends on the demand (arrival) and the supply (transmission success), formally $p_l(t) \times \mu_l(t) = \exp(q_l(t))$. Together with this parameter control, the source rate control by $U'^{-1}(q(t)/V)$, where $U(\cdot)$ is a utility function, ensures that the long-term throughput is the solution of network utility maximization (NUM) problem. By suitably choosing the form of the utility function, we can achieve various fairness criteria. In this paper, we focus on $U(\cdot) = \log(\cdot)$ (thus, $U'^{-1}(q(t)/V) = V/q(t)$).

We highlight that O-DCF is not just a naive implementation of oCSMA because: 1) many assumptions in the oCSMA theory, e.g., no collisions in the continuous time framework, symmetric sensing, perfect channel holding, etc., do not hold in practice. 2) Furthermore, O-DCF is constrained to be fully compatible with 802.11 chipsets. 3) More importantly, in theory, any combination of p_l and μ_l works well as long as their product is $\exp(q_l)$. However, we need to find a careful combination of them for high performance in practice. All of these issues will be elaborated in the following sections.

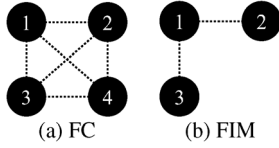


Fig. 2. Example topologies' conflicting graphs. Vertices are the links in interference graphs; dotted lines represent interference. (a) FC with four links. (b) FIM with two outer links.

B. Tension Between Symmetric and Asymmetric Contention

1) *Topological Dependence*: A good combination of two CSMA operational parameters for high performance depends on contention topologies. O-DCF is designed to *autonomously* choose the combination of access probability and transmission length without explicit knowledge of topological information. Just for ease of explanation, we provide our description, assuming that flows are configured in either of the two “extreme” topologies: fully connected (FC) for symmetric contention and flow-in-the-middle (FIM) for asymmetric contention (see Fig. 2), but O-DCF generally works well beyond these two topologies. Recall the two key design ideas of O-DCF: We first choose the initial access probability as a sigmoid function of the queue length and then let it experience BEB. To summarize, BEB is a key component in symmetric contention and the sigmoid function-based access probability selection is crucial in asymmetric contention, and both are important in “mixture” topologies (all of which are presented below, respectively).

2) *O-DCF: How Exponential Backoff Helps*: In symmetric contention, the access probabilities among the contending flows should be reasonably low; otherwise, throughput will naturally degrade. Note that to guarantee fairness and high (long-term) throughput, a tiny p_l can work as it leads to almost no collision. This is because in that case a significantly long transmission length would recover the long-term throughput, as explained in oCSMA theory. However, such a combination will lead to a serious problem in short-term fairness, where a maximum bound on transmission length to guarantee short-term fairness is enforced in practice. For an automatic adaptation to contention level, we utilize BEB as a *fully distributed search process* for the *largest* access probability (i.e., the smallest CW size) that lets the links share the media efficiently in presence of collisions.

3) *O-DCF: Why Sigmoid Function*: As opposed to symmetric contention, in asymmetric contention such as FIM-like topologies, almost no collision occurs, and thus BEB rarely operates (we confirmed in Section VI-B). More importantly, in this case, the starvation of the central flow is a major issue. To tackle this, we require that the CW size (or the access probability) of link l that solely contends with many other links should be *small* (or *high*) and thus *prioritized* enough that the link l avoids rare channel access and even starvation. To provide such *access differentiation*, we focus on the fact that the flow in the middle, say l , typically has a longer queue than the outer flows. Let us denote the access probability p_l by some function of queue length q_l , i.e., $p_l = f(q_l)$. Thus, it is natural to design $f(q_l)$ to be *increasing* for access differentiation.

The question is what form of the function $f(q_l)$ is appropriate for high performance. To streamline the exposition, we proceed the discussion with the access probability rather than the CW.

Toward efficient access differentiation, we start by the f 's requirements: For any link l and for $q_{\min} \leq q \leq q_{\max}$:

- R1) $0 \leq f(q_l) \leq \bar{p} < 1$, where $f(q_{\min}) \approx 0$ and $f(q_{\max}) = \bar{p}$. The largest access probability \bar{p} should be strictly less than one to prevent channel monopolization.
- R2) $[f(q_l)]_2^8$ should span all the values in $\{1/2^i, i = 0, \dots, 9\}$, each of which corresponds to the CW sizes $\{2^{i+1} - 1, i = 0, \dots, 9\}$.
- R3) The transmission lengths of the flows with heavy contention and those with light contention should be kept small not to exceed maximum aggregation size/time.

The requirement R3 is important to prevent the central flow from being starved. In the FIM-like topologies, the flows experiencing heavy contention such as the central one in FIM has very rare chances to access the media. To guarantee (proportional) fairness, it is necessary for such flows to select long transmission lengths whenever holding the channel. However, as mentioned earlier, the transmission length should be bounded with the maximum aggregation size and/time for practical purposes such as short-term fairness. This implies that the central flow often needs to stop the transmissions before its required transmission length for optimal fairness is reached. Efficient flow differentiation, which prioritizes the flows with heavy contention in terms of access probability, significantly helps by reducing the required transmission length with a reasonable value (mostly shorter than the maximum transmission length) towards long-term fairness. An extreme case for asymmetric contention is IA scenario where two flows have asymmetric interference relationship. We will explain in Section V-C that our flow differentiation helps a lot in providing (long-term) fairness in such a problematic scenario.

An intuitive way to realize flow differentiation is to set the access probability of link l to be $\exp(q_l)/K$ for some constant K . Then, the rule (7) enforces the transmission length to be around K , *irrespective of the contention levels of the flows* (i.e., R3). However, to satisfy R1, we use a slightly different function that has a sigmoidal form, $f(q_l) = \exp(q_l) / (\exp(q_l) + C)$, with some constant C . This function naturally makes the chosen access probability to be strictly less than one for any $q_{\min} \leq q \leq q_{\max}$, unlike $\exp(q_l)/K$. Clearly, the sigmoid function is not exponential over the entire $q_{\min} \leq q_l \leq q_{\max}$ values. However, it suffices to have an exponential form up to q'_l with $f(q'_l) = 0.75$, since for a larger $q_l > q'_l$, the CW size approaches one from the CW granularity (but the access probability is set to be strictly less than one).

Then, the next question is the inflection point, determined by the constant C . We choose C around 500 due to the following reasons. First, for the resultant p to span the whole feasible values (as in R2), C should be greater than 500, i.e., $f(q_{\min}) = (\exp(q_{\min}) / \exp(q_{\min}) + 500) \approx (1/512)$, where $q_{\min} = bQ_{\min} = 0.01$ [see Fig. 3(b) in terms of CW]. Second, the parameter C determines the location of inflection point in the sigmoid function. For example, let us consider the FIM topology with four outer flows, where the central flow can have its queue length of up to five, while the outer flows have much smaller queue lengths usually less than two. To guarantee the exponential increase in that curve, the x -axis at the inflection point should be larger than five, implying that C larger than

⁸We denote by $[x]_2$ the $1/2^i$ for some integer i , which is closest to x , e.g., $[0.124]_2 = 1/2^3$ and $i = 3$.

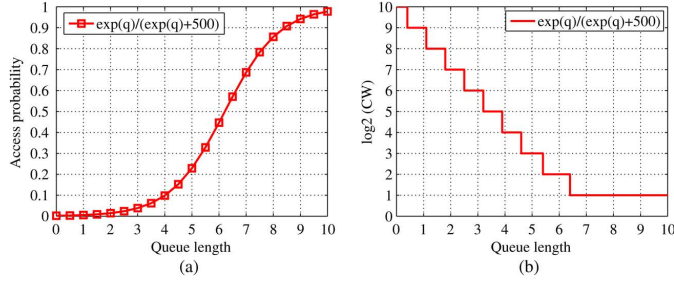


Fig. 3. Illustration of sigmoid function with respect to queue length. (a) Queue versus p . (b) Queue versus CW .

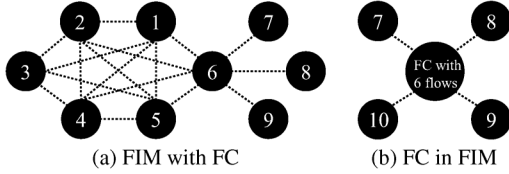


Fig. 4. Mixed topologies' conflicting graphs. (a) The flow 6 belongs to both FC and FIM topologies. (b) six flows within a FC group form a FIM topology with four outer flows.

500 is sufficient since $f(5) = (\exp(5)/\exp(5)500) < (1/2)$. However, too large C values directly result in too long transmission lengths from (7) because they may yield very low p 's.

4) *Mixture of Contention Levels*: In practice, it is possible for a link to appear in a mixture of topologies with symmetric and asymmetric contention. We study this issue using the example scenarios in Fig. 4. First, in Fig. 4(a), flow 6 interferes with flows 1, ..., 5 in a fully connected fashion, and also with flows 7–9 in a FIM-like fashion. Since it senses the transmission of both the remaining links forming the FC group and outer links forming the FIM group, its queue temporarily builds up, thus having a larger access probability than outer links due to the sigmoidal curve. However, it shares the medium equally with others in FC group so that their queue lengths increase together. Thus, in the worst case, BEB can prevent too aggressive access among the links within FC group. More importantly, *even the reduced access probability from BEB is kept larger than those of outer links* (see Section VI-B for simulation results), thus still being sufficiently prioritized in the FIM topology, preserving proportional fairness. Similar trends are also observed in Fig. 4(b).

5) *Aggressiveness Control for Session Tails*: Sessions dynamically enter and leave over time. As sessions' packets are served in a node (without new session arrivals), the CQ size naturally decreases, resulting in progressively less aggressive media access. In O-DCF, as the CQ size becomes zero, we record the MAQ size at that time and access the media with the recorded MAQ size (not actual MAQ size) until all the packets at MAQ are served. This effectively solves the problem that the session tails may be processed with too low aggressiveness.

C. Imperfect Sensing and Capture Effect

We have so far described O-DCF for the perfect sensing case. However, sensing is often imperfect, as illustrated in Fig. 5. RTS-CTS-like virtual sensing in O-DCF is not a complete solution because just a naive choice of access probability and transmission length may generate a self-feeding loop where collisions increase queue lengths, which in turn leads to

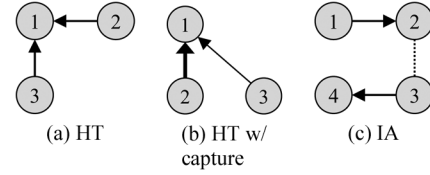


Fig. 5. Example topologies of imperfect sensing and packet capture. In network graphs, vertices represent nodes, dotted lines represent connectivity, and arrows represent flows. (a) HT. (b) HT with capture. (c) IA: a thin arrow for weak signal.

more aggressive access and thus heavier collisions, especially under the CW adaptation (defined in Section VI-A) [25]. Our queue-based initial CW with BEB substantially lessens such bad impacts. In *HT*, if the queue lengths of hidden nodes are large, BEB lets each node increase its CW, so that with small time cost, a transmission succeeds. This successful transmission generally decreases the queue lengths, preventing CW from being too small due to queue-based initial CW selection. In *IA*, collisions are asymmetric. Suppose that at some time, advantaged and disadvantaged flows have small and large queue lengths, respectively. Then, the disadvantaged flow will have a smaller initial CW, thus leading to successful transmissions and simultaneously the advantaged flows will hear CTS signalling (responding to RTS from the disadvantaged flow) and stop their attempts. This helps a lot in providing fairness between two asymmetric flows. The packet capture effects can be handled by our method similarly to the *IA* scenario, i.e., interference asymmetry. For example, in *HT with capture*, similar behaviors to the *IA* case occur between weak and strong nodes.

D. O-DCF Implementation

1) *Queue Structure*: We implemented O-DCF as an overlay MAC on legacy 802.11 hardware using our C-based software platform, which requires protocol implementation on top of MadWiFi device driver [34]. Due to a limited memory size of legacy network interface card (NIC), we implement CQ and MAQ at the user space level. Note that the scheduling from MAQ to IQ is not an actual packet transmission to the media. To minimize the temporal gap between the service from MAQ and the actual transmission, we reduce the buffer limit of IQ to a small value (e.g., 10) through a device driver modification. Note that timely ack transmissions are still maintained by our O-DCF implementation since those are processed immediately at the firmware of 802.11 hardware without being enqueued into MAQ and IQ.

2) *O-DCF Scheduler and Parameter Control*: A scheduler in O-DCF schedules the packets enqueued at MAQ to send them into the 802.11 hardware, as shown in Fig. 1. Whenever IQ in 802.11 becomes empty, the scheduler in O-DCF is notified by a system call such as `raw socket` function and determines the next packet to be enqueued into IQ by comparing the lengths of multiple per-neighbor MAQs. Meanwhile, the scheduler maintains CSMA parameters, such as CW, AIFS, and NAV values, for each MAQ's HOL packet. To facilitate packet-by-packet parameter control, we piggyback such parameters into the header of HOL packet, so that the modified driver can interpret and set them in the TXQ descriptor of an outgoing packet for the actual transmission.

3) *Long Data Transmission*: When packet aggregation is not supported in legacy 802.11 hardware, as in our real

testbed, such as 802.11a/b/g, we take the following approach. The O-DCF scheduler assigns different arbitration interframe spaces (AIFSs) and CWs for packets inside the specified transmission length. Since AIFS defines a default interval between packet transmissions and the smallest CW indicates the shortest backoff time, this provides a prioritization for *back-to-back* transmissions until the given transmission length expires. Furthermore, we exploit the network allocation vector (NAV) option that includes the time during which neighbors remain silent irrespective of sensing. This guarantees that even interfering neighbors unable to sense (due to, e.g., channel fluctuations) do not prevent the transmission during the reserved transmission length.

4) *Link Capacity Update*: As discussed in Section IV-D, to exploit multirate capability, we need to get the runtime link capacity information from the device driver. To fetch the runtime capacity, we periodically examine `/proc` filesystem in Linux. The period has some tradeoff between accuracy and overhead. We employ the exponential moving average each second to smooth out the channel variations as well as to avoid too much overhead of reading `/proc` interface.

VI. PERFORMANCE EVALUATION

A. Setup

Environment: We use both NS-3 simulation and real experiments on a 16-node wireless testbed. The simulations are conducted for the basic topologies as well as the topologies that are hard to manually configure in the real experiments. We perform testbed experiments for the topologies randomly made in a building as well as the topologies that are more sensitive to the real environments such as packet capture. The details of our testbed specification will be described in Section VI-C. For all scenarios, we repeat 10 times (each lasting for 100 s) and measure the goodput at receiver, and the length of error bars in all plots represents standard deviation. The packet size is 1000 B. The parameters used in O-DCF are as follows: The queue scaling constant $b = 0.01$, the queue bounds are $Q_{\min} = 1$, $Q_{\max} = 1000$, and $V = 500$ (recall that the dequeue rate from CQ to MAQ is $V/q_l^M(t)$). We consider fully backlogged flows in most scenarios, except for one plot that shows how O-DCF works for dynamic session arrival and departure. See Section VII for our parameter choices and other evaluation results. Our NS-3 simulation codes are publicly available in [35].

Tested Protocols: We compare: 1) 802.11 DCF; 2) two versions of oCSMA in theory; and 3) DiffQ [7]. For the standard oCSMA, we test two versions (to show the effect of our automatic CSMA parameter combination in O-DCF: 1) *CW adaptation* in which we typically fix the transmission length μ with a single packet and control the access probability $p_l(t)$, such that $p_l(t) \times \mu = \exp(q_l(t))$ [1]; and 2) μ adaptation with BEB (simply μ adaptation in this paper) in which we delegate the selection of $p_l(t)$ to 802.11 DCF and control $\mu_l(t) = \exp(q_l(t))/p_l(t)$. Note that to understand the effect of different methods for the adaptation of CWs, we evaluate μ adaptation with BEB using 802.11's CW size, and compare it to O-DCF. DiffQ is a *heuristic* queue-based MAC based on the 802.11e feature and schedules the interfering links with different priorities based on queue lengths.

CW- and μ -Adaptation Implementation: In CW adaptation, we first fix the transmission length with a packet size of 1000 B,

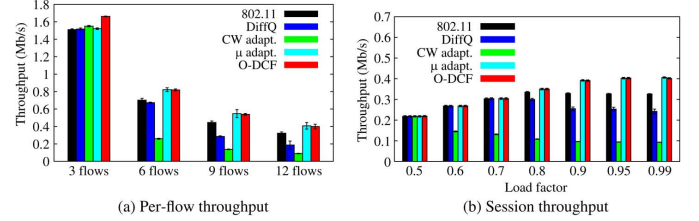


Fig. 6. (a) Average throughput in FC with 3, 6, 9, and 12 fully backlogged flows (b) Session throughput for dynamic (thus, unsaturated) traffic.

and change CW size based on the access probability of each link. This implementation setting is already used by prior work, e.g., [1] and [25]. In μ adaptation, the value of fixed CW size has large impact on the performance, set by the following guideline: Note that too large CW sizes require significantly long transmission lengths, thus often upper-limited by the maximum transmission length, whereas too small CW sizes result in aggressive channel accesses, suffering from low throughput due to excessive collisions, as analytically studied in [36]. We do not change the default CW size (i.e., $CW = 16$ slots) as in 802.11 DCF, but we allow μ adaptation to find a proper CW value through BEB mechanism, so that it operates as much as possible within the bounded access aggressiveness range. For fair comparison, those two oCSMA variants share the overall architecture (e.g., MAQs and CQs) and the access aggressiveness control procedure with O-DCF. We expect that such an architecture is needed in any practical MAC protocol motivated by per-neighbor queue-based MAC from theory.

B. Simulation Results: Basic Topologies

1) *Fully Connected: Impact of Contention Degrees*: Fig. 6(a) summarizes the average per-flow throughput for the FC topologies [see Fig. 2(a)] for varying contention levels. The key point here is that O-DCF performs well *regardless* of the contention levels. All algorithms are good for the small number of flows. However, with increasing contention levels, the throughputs of DiffQ, 802.11, and CW adaptation decrease. μ adaptation performs similarly to O-DCF because in FC, they transmit multiple packets by enlarged transmission length after backing off with proper CW size adjusted by BEB. 802.11's bad performance in many-flow case is because the flows are unconditionally aggressive, where O-DCF's initial access probability is adapted over time. CW adaptation reveals the worst performance with more than six flows since it increases access probability too much in the case of high contentions, which leads to frequent collisions.

2) *FIM: Impact of Contention Asymmetry*: Next, we study the case of asymmetric contention, using the FIM topology [see Fig. 2(b)]. Fig. 7 shows that O-DCF and CW adaptation dominate other algorithms. We observe that collisions are rare (less than 10%⁹ in simulation, less than 2% in experiment), and thus BEB hardly happens. As reported in other papers [7], [9], the central flow experiences serious starvation in 802.11. In contrast to the symmetric contention as in FC, μ adaptation with BEB leads to the starvation of the central flow since outer flows

⁹This seems quite high, but the reason is that the total number of transmission attempts at central flow is small. Thus, the absolute number of collisions is small.

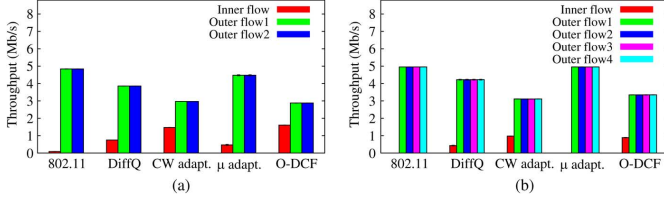


Fig. 7. FIM topology with two and four outer flows. In (a) and (b), the ideal proportional-fair throughput ratios of an outer flow and a middle flow are: 2:1 and 4:1, respectively. (a) Two outer flows. (b) Four outer flows.

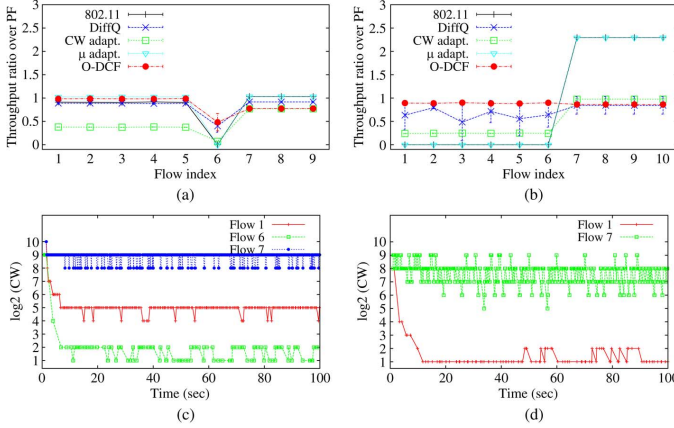


Fig. 8. Simulation. (a), (b) Performance comparison in two mixed topologies; the flow indexes are the same as in Fig. 4; we plot the throughput ratio over optimality: The closer to one the ratio is, the better fairness is. (c), (d) CW traces of representative flows are plotted over time in O-DCF. (a) FIM with FC (9 flows). (b) FC in FIM (10 flows). (c) CWs of O-DCF in “FIM with FC” topology. (d) CWs of O-DCF in “FC in FIM” topology.

use 802.11’s small CW to access the channel due to few collisions, which is too short to have enough overlapping of silent times and let the central flow transmit. Thus, in O-DCF, we can adapt the transmission length μ with a smarter CW selection method for high fairness. DiffQ resolves the starvation of the central flow well, but it shows suboptimal performance due to the heuristic setting of CW size.

3) *Mixed Topology*: We now consider the case when some flows belongs in part to symmetric and asymmetric contention (see Fig. 4). Fig. 8(a) shows the normalized per-flow throughput by the optimal PF share over the topology in Fig. 4(a). We observe that O-DCF outperforms others in terms of fairness. Note that the flow 6 placed between two different contention patterns experience some suboptimal fairness. This is because flow 6 should have low access probability due to the contention with flows 1–5, but it should also be prioritized over the flows 7–9. Our result shows that despite such conflicting situations, O-DCF tries to adjust the access probability and set the transmission length, so that the fairness is sustained to be reasonable, whereas other algorithms suffer from bad fairness. This is indeed achieved by our queue-length-based initial CW selection with BEB in a distributed manner, which is verified by Fig. 8(c). Similar principles are applied to the topology in Fig. 4(b), whose (normalized) per-flow throughput and CW traces are shown in Fig. 8(b) and (d), respectively.

4) *Dynamic Traffic*: In addition, we evaluate the case with bursty traffic where active flow sessions can dynamically arrive or leave the system. In a fully connected topology with 12 flows, we generate multiple active sessions, each of them transferring

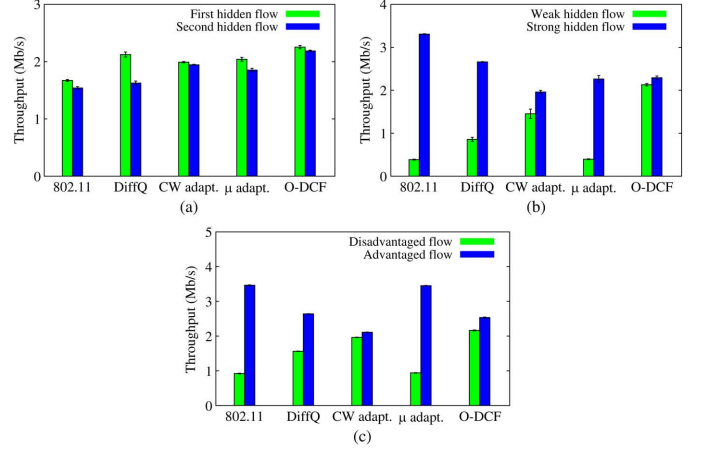


Fig. 9. Performance comparison in HT without packet capture (*top left*) and with packet capture (*top right*), and IA (*bottom*) topologies. (a) HT w/o cap. (b) HT w/cap. (c) IA.

a file of 1 MB size. The results are shown in Fig. 6(b) for different system load values. To obtain different load levels, we vary the session interarrival times, which is $1 \text{ MB} / (5.4 \text{ Mb/s} \times \text{load factor}) \times 12$. Then, we evaluate system throughput versus load as shown in the figure. We observe that, when the network load is low, all protocols can satisfy the flow traffic demands (see the case with load factor 0.5), and therefore all protocols have similar performance. However, as the load in the network increases, the system starts behaving in a more similar way to the fully backlogged case, accumulating packets at the MAC layer queues as traffic demands overload system capacity. As an extreme case, for a network load of 0.99, we observe a very similar performance for all protocols to the one in Fig. 6(a) (i.e., the fully backlogged case). In conclusion, with bursty traffic, low demands are easy to satisfy by any of the protocols, but with bursty traffic and higher demands, the benefits in the use of O-DCF become more evident and are comparable to the ones already explained for the fully backlogged case.

C. Experiments

In our 16-node testbed, each node is a netbook platform (1.66 GHz CPU and 1 GB RAM) running Linux kernel 2.6.31 and equipped with a single 802.11a/b/g NIC (Atheros chipset) running the modified MadWiFi driver for O-DCF’s operation. To avoid external interference, we select a 5.805-GHz band in 802.11a. The default link capacity is fixed with 6 Mb/s, but we vary capacity or turn on auto rate adjustment, if needed.

1) *Imperfect Sensing and Capture Effect*: We investigate the impact of imperfect sensing in O-DCF with the topologies: HT, IA, and HT with capture, which are depicted in Fig. 5. As discussed in Section V-C, we enable a virtual sensing, i.e., RTS/CTS signaling by default for better channel reservation before data transmission in all tested algorithms. Fig. 9 shows the throughput results for the three topologies, respectively. First, in HT, O-DCF outperforms others in symmetric interference conditions by hidden nodes, as well as asymmetric conditions due to packet capture. Particularly, in O-DCF, collisions and thus BEB allow the hidden flows to access the media with larger CWs (i.e., less aggressiveness), resulting in many successful RTS/CTS exchanges. Fairness is guaranteed by the transmission length control. Second, in IA, our O-DCF shows very fair and high throughput, where the advantaged flow has a larger

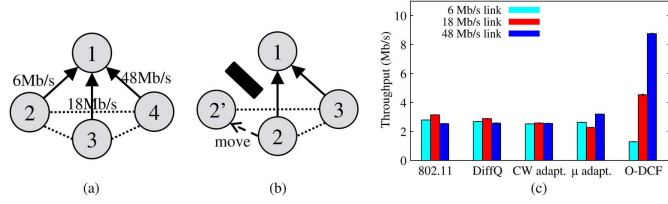


Fig. 10. Experiment. Single-hop network scenario consisting of clients and one AP. (a) Static case: All nodes remain fixed with different PHY rates. (b) Mobile case: Node 2 moves away from node 1 at 60 s. (c) Per-flow throughput.

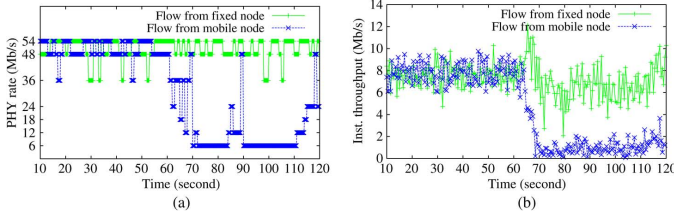


Fig. 11. Experiment. Performance evaluation in mobile scenario [Fig. 10(b)]. (a) Runtime PHY rate. (b) O-DCF w/rate update.

CW due to small backlog, and the disadvantaged flow also uses a larger CW due to BEB, responding well to collisions. As a result, both flows contend with sufficiently large CW values without heavy collisions, enjoying better RTS/CTS-based medium reservation. Similarly, we can ensure fairness in the scenario with packet capture. In μ adaptation, the advantaged flow accesses the channel using 802.11's small CW due to few collisions, which leads to a high probability of collisions and even starvation of the disadvantaged flow, and thus unfairness between two flows deepens. DiffQ cannot solve unfairness perfectly due to the still aggressive CW values. However, CW adaptation grants more aggressiveness to less-served flows, thus reducing the throughput gap between two flows in those scenarios, while still leaving a small gap from optimality.

2) *Heterogeneous Channels*: We consider two scenarios: 1) *static* in Fig. 10(a): Nodes are stationary with different link rates, 6, 18, and 48 Mb/s; and 2) *mobile* in Fig. 10(b): Each node turns on the auto-rate functionality and two clients send their data to a single AP, and after 60 s, one of two clients (say node 2) moves away from AP (node 1). In adapting the rate, we employ the famous SampleRate algorithm [30] in MadWiFi driver. We measure the runtime PHY rate information updated every 1-s interval. First, in the static scenario, as shown in Fig. 10(c), we observe that only O-DCF can attain proportional fair rate allocation in an efficient manner, because of the consideration of link rate heterogeneity in the choice of CWs and transmission lengths, whereas the other protocols show severe inefficiency that the flows with higher rates are significantly penalized by that with lower rate. Besides the long-term fairness study in the static scenario, we examine the responsiveness of O-DCF to channel variations in the mobile scenario, shown in Fig. 11(a). We trace the instantaneous throughput of both fixed and mobile nodes in Fig. 11(b), where we see that the incorporation of the runtime PHY rate in O-DCF indeed helps in achieving throughput efficiency instantaneously even in the auto-rate enabled environment.

3) *Random Topology Experiment in a Building*: We now conduct a more general experiment using a 16-node testbed topology, as shown in Fig. 12(a), where we test two cases of

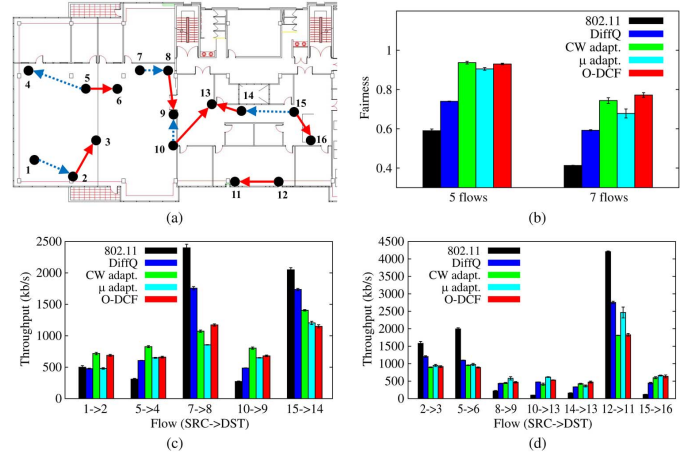


Fig. 12. Experiment. Tested topology and performance comparison. (a) Tested scenario of 16 nodes denoted by triangles are distributed in the area of 40×20 m²; dotted (solid) arrows represent 5 (7) flows for the first (second) scenario. (b) Jain's fairness comparison. (c) Per-flow throughput distribution of 5 flows. (d) Per-flow throughput distribution of 7 flows.

five and seven concurrent flows. This random topology enables us to see how the algorithms perform in the mixture of hidden terminals and heavy contention scenarios including FIM scenario. Fig. 12(b) compares Jain's fairness achieved by all the algorithms for two scenarios. We find that over all the scenarios, O-DCF outperforms others in terms of fairness (up to 87.1% over 802.11 and 30.3% over DiffQ), while its sum utility is similar with others. The fairness gain can be manifested in the distribution of per-flow throughput, as shown in Fig. 12(c) and (d). O-DCF effectively prioritizes the flows with more contention degree (e.g., flow $10 \rightarrow 9$ forms *flow-in-the-middle* with flows $7 \rightarrow 8$ and $15 \rightarrow 14$) and provides enough transmission chances to highly interfered flows (i.e., $8 \rightarrow 9$, $10 \rightarrow 13$, and $14 \rightarrow 13$), compared to 802.11 DCF and DiffQ. The experimental topology is somewhat limited in size, tending to be fully connected. This leads to a small performance gap between oCSMA and O-DCF, but 802.11 DCF yields severe throughput disparities of more than 40 times between flows $12 \rightarrow 11$ and $10 \rightarrow 13$ in the second scenario. Compared to 802.11, DiffQ performs fairly well in the sense that it prioritizes highly interfered flows. However, its access prioritization is heuristic, so there is still room for improvement compared to O-DCF.

D. Simulation Results: Large Topologies

Finally, we extend the evaluation of O-DCF to three large-scale scenarios, which are artificially or randomly configured and come from a real operational network. The first is a *grid network* where 16 nodes are apart from each other with 250 m, and the second is a *random network* where 30 nodes are deployed randomly within an area of 1000×1000 m². These networks, depicted in Fig. 13(a) and (b), contain a mixture of the previously discussed problematic scenarios, such as HT, IA, and FIM, as well as highly interfering FC groups. We also add the third scenario that deals with the *technology for all (TFA) mesh network* [37], which is an operational network with 21 nodes deployed in an area of 3 km² in Houston, TX, USA. Using the coverage map of TFA [37], we construct its network topology based on the link connectivity information. For a given number of flows, we construct 10 scenarios with different random single-hop flows. In particular, we simulate

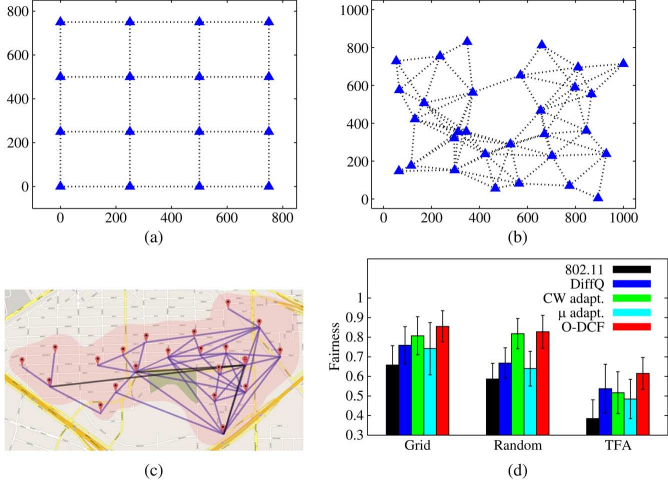


Fig. 13. Simulation. Large-scale topologies within wide areas (1 km^2 for grid and random, and 3 km^2 for TFA). In grid and random topologies, each node denoted by triangles has transmission and sensing ranges equal to 280 m. (a) Grid topology: 16 nodes form a grid network. (b) Random topology: 30 nodes are deployed randomly. (c) TFA topology: 21 nodes are deployed in operational TFA network. (d) Jain's fairness: fairness comparison among tested algorithms.

6, 12, and 10 flows over grid, random, and the TFA networks, respectively.

Fig. 13(d) compares the Jain's fairness achieved by five algorithms in all three network scenarios. O-DCF enhances fairness up to 59.8% (resp., 41.0% and 29.9%) over 802.11 DCF and 14.6% (resp., 24.0% and 12.6%) over DiffQ in the TFA (resp., random and grid) network. Since the TFA network has higher contention level than grid and random networks, CW adaptation suffers more from collisions as explained in Section VI-B. Compared to the previous experiments, we observe more throughput disparities of contending flows under DiffQ and μ adaptation. In most scenarios, randomly chosen flows likely have problematic relationships such as HT and IA. This leads to lower fairness of DiffQ and μ adaptation than O-DCF and CW adaptation since they are vulnerable to imperfect sensing scenarios, as examined in Section VI-C.1.

VII. TOWARD PRACTICAL O-DCF

A. Parameter Selection

The parameters of O-DCF are as follows: b , Q_{\min} , Q_{\max} , and V . The value of b can be chosen by a typical step-size in many of optimization algorithms, say 0.01 or 0.001. The queue bound parameters Q_{\min} and Q_{\max} are rather important because $Q_i^M(t)$ is used to determine the injection rate from CQ to MAQ (i.e., $V/(bQ_i^M(t))$), linked to the access aggressiveness. Thus, Q_{\min} and Q_{\max} are chosen just to avoid too small or large injection rates. Finally, it is intuitive that larger V leads to more sensitive response to the changes of $Q_i^M(t)$. This intuition has been proven in theory that V controls a tradeoff between long-term throughput and queueing delay, e.g., [38]. Our simulations for FC and FIM topologies (see Figs. 14 and 15, respectively) verify such a tradeoff. To elaborate, in case of FC topology with three flows, we observe that there exists some gain in throughput with the increasing value V at the cost of increasing queueing delay. However, in case of FC topology with more flows (≥ 6), there is no gain in throughput even with larger V since wireless channel resource is already saturated by many contending

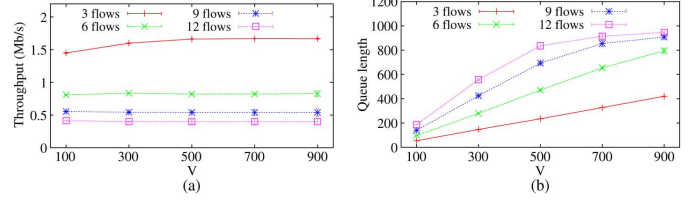


Fig. 14. Simulation of O-DCF. FC topology with 3, 6, 9, and 12 flows for different values of V . (a) Per-flow throughput. (b) Queue length.

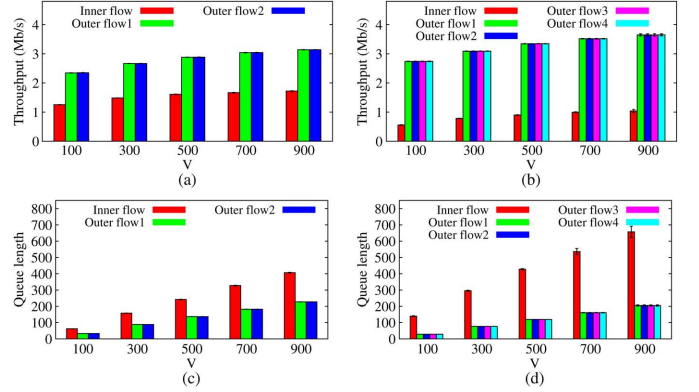


Fig. 15. Simulation of O-DCF. FIM topology with two and four outer flows for different values of V . (a) Two outer flows. (b) Four outer flows. (c) Queue length for two outer flows. (d) Queue length for four outer flows.

flows, whereas in case of FIM topology with two and four outer flows, larger V leads to throughput increase for all flows together with queueing delay increase since wireless channel resource still leaves some room.

B. Inter-TX Time: Short-Term Fairness

It is natural that enlarged transmissions in O-DCF sometimes increase the inter-TX delay of some flows (i.e., jitter). To limit the increasing jitter, we adopt the maximum transmission length specified by 802.11n standard, i.e., 10 ms in time (or 64 kB in size). The maximum transmission length tends to be shorter, as 802.11 PHY is enhanced. Also, even in such a worse case, O-DCF still keeps substantial benefits in terms of long-term fairness. This confirms the results of prior work [3], [24], which has shown a tradeoff between short-term fairness and long-term efficiency in oCSMA algorithms. More importantly, the performance benefits in O-DCF can be found in critical scenarios where other CSMA protocols fail to achieve fairness, as shown in the previous sections.

C. Coexisting With 802.11 DCF

We now discuss when O-DCF coexists with 802.11 DCF. The important of this study lies in despite the physical-layer enhancement of IEEE 802.11 technology (e.g., 802.11ac), 802.11 DCF is still being widely used as a basic MAC protocol in practice, and a widely used MAC is rarely replaced by a new MAC. Differently from O-DCF, 802.11 DCF does not change its access aggressiveness, given that the transmitted packet size is constant, since it uses a fixed backoff time (randomly chosen from a fixed CW value) and activates BEB in response to packet collisions. However, O-DCF adapts its access aggressiveness according to contention level in the neighborhood indirectly quantified by the local queue length. Thus, contending between both

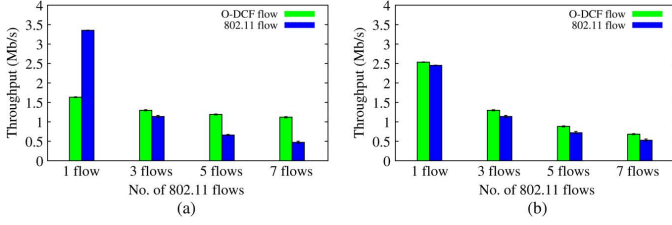


Fig. 16. Simulation. FC topology with varying number of 802.11 flows and one O-DCF flow. (a) O-DCF with $V = 500$. (b) O-DCF with V control.

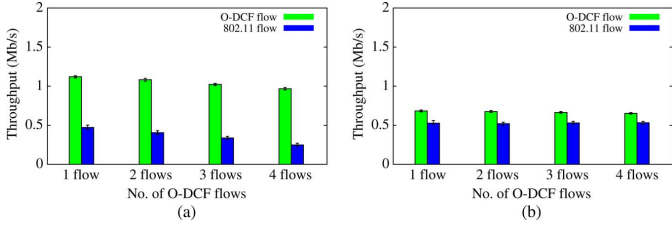


Fig. 17. Simulation. FC topology with varying number of O-DCF and 802.11 flows. However, total number of flows is equal to eight. (a) O-DCF with $V = 500$. (b) O-DCF with V control.

protocols in the same collision domain definitely results in starvation of 802.11 DCF as their contention level grows.

A method of providing fairer channel access to both protocols would be to equalize both protocols' aggressiveness based on the contention level. In particular, O-DCF needs to adjust its aggressiveness properly since 802.11 DCF cannot change the aggressiveness. To this end, we propose to control V parameter based on the number of contending flows. We set the initial value of V such that O-DCF achieves the same throughput as 802.11 DCF does. In our simulation, for $V = 2000$, O-DCF achieves the same as 802.11 DCF (e.g., 5 Mb/s at 6 Mb/s link). Now, we revisit (1) to control V . In steady state, the queue length would not change, thus $A_l \approx S_l$, where $A_l = V/q_l$ under log utility function and $S_l = C/N$ in FC topology with link capacity C and N flows. As N increases, we decrease V , so that O-DCF keeps its aggressiveness similarly as 802.11 DCF has a fixed one. We assume that O-DCF transmitter is capable of knowing the number of contending flows.¹⁰ We evaluate this proposed scheme by performing simulation in the FC topology.

Fig. 16 compares throughput performance of O-DCF and 802.11 DCF. We only depict one of multiple 802.11 flows for clear comparison (in fact, the result shows a fair share among 802.11 flows). When contention level is small (i.e., two flows in FC), 802.11 operates more aggressively than O-DCF, so it attains two times more than O-DCF. However, as the number of 802.11 flows increases in the network, O-DCF raises its aggressiveness, thus surpassing 802.11 beyond more than three 802.11 flows. However, with V control, O-DCF flow can share the medium with 802.11 flows fairly since it reduces the aggressiveness in response to growing contention level. We also consider a greedy scenario when the number of O-DCF flows increases gradually up to that of 802.11 ones. Fig. 17 shows the result in that scenario. We observe that 802.11 flows can be

starved more seriously by multiple greedy O-DCF flows. However, our V control comes into play irrespective of the number of O-DCF flows, thus making both MACs share the medium in a fair manner. Note that total throughput of both cases (i.e., with and without V control) is almost the same, meaning that V control cannot severely affect throughput optimality in O-DCF.

VIII. CONCLUSION

The major design issues to improve 802.11 DCF are contention window selection and transmission length control against network contention, imperfect sensing, channel heterogeneity, and packet capture without any message passing. We proposed a protocol, called O-DCF, inspired by the recent theory on CSMA to tackle these issues. However, we highlight that our work is not just an implementation of what has been developed in theory, covering many important engineering optimizations that have large impacts on the actual performance and deployment in practice. This paper shows that a combination of effective design ideas and implementation choices can actually let a theory-motivated protocol applicable in practice. We hope that our paper encourages and motivates other follow-up work to further bridge the gap between practice and theory.

REFERENCES

- [1] L. Jiang and J. Walrand, "A distributed CSMA algorithm for throughput and utility maximization in wireless networks," *IEEE/ACM Trans. Netw.*, vol. 18, no. 3, pp. 960–972, Jun. 2010.
- [2] S. Rajagopalan, D. Shah, and J. Shin, "Network adiabatic theorem: An efficient randomized protocol for contention resolution," in *Proc. ACM SIGMETRICS*, 2009, pp. 133–144.
- [3] J. Liu, Y. Yi, A. Proutiere, M. Chiang, and H. V. Poor, "Towards utility-optimal random access without message passing," *Wireless Commun. Mobile Comput.*, vol. 10, no. 1, pp. 115–128, Jan. 2010.
- [4] J. Ni, B. Tan, and R. Srikant, "Q-CSMA: Queue-length based CSMA/CA algorithms for achieving maximum throughput and low delay in wireless networks," in *Proc. IEEE INFOCOM*, 2010, pp. 1–5.
- [5] P. Marbach and A. Eryilmaz, "A backlog-based CSMA mechanism to achieve fairness and throughput-optimality in multihop wireless networks," in *Proc. Allerton Conf.*, 2008, pp. 768–775.
- [6] D. Skordoulis et al., "IEEE 802.11n MAC frame aggregation mechanisms for next-generation high-throughput WLANs," *IEEE Wireless Commun.*, vol. 15, no. 1, pp. 40–47, Feb. 2008.
- [7] A. Warrier, S. Janakiraman, S. Ha, and I. Rhee, "DiffQ: Practical differential backlog congestion control for wireless networks," in *Proc. IEEE INFOCOM*, 2009, pp. 262–270.
- [8] V. Bharghavan, A. Demers, S. Shenker, and L. Zhang, "MACAW: A media access protocol for wireless LANs," in *Proc. ACM SIGCOMM*, 1994, pp. 212–225.
- [9] M. Garetto, T. Salonidis, and E. Knightly, "Modeling per-flow throughput and capturing starvation in CSMA multi-hop wireless networks," in *Proc. IEEE INFOCOM*, 2006, pp. 1–13.
- [10] X. Wang and K. Kar, "Throughput modelling and fairness issues in CSMA/CA based ad-hoc networks," in *Proc. IEEE INFOCOM*, 2005, pp. 23–34.
- [11] S.-J. Han, T. Nandagopal, Y. Bejerano, and H.-G. Choi, "Analysis of spatial unfairness in wireless LANs," in *Proc. IEEE INFOCOM*, 2009, pp. 2043–2051.
- [12] M. Heusse, F. Rousseau, G. Berger-Sabbatel, and A. Duda, "Performance anomaly of 802.11b," in *Proc. IEEE INFOCOM*, 2003, pp. 836–843.
- [13] F. Cali, M. Conti, and E. Gregori, "Dynamic tuning of the IEEE 802.11 protocol to achieve a theoretical throughput limit," *IEEE/ACM Trans. Netw.*, vol. 8, no. 6, pp. 785–799, Dec. 2000.
- [14] M. Heusse, F. Rousseau, R. Guillier, and A. Duda, "Idle Sense: An optimal access method for high throughput and fairness in rate diverse wireless LANs," in *Proc. ACM SIGCOMM*, 2005, pp. 121–132.
- [15] V. A. Siris and G. Stamatakis, "Optimal CWmin selection for achieving proportional fairness in multi-rate 802.11e WLANs: Test-bed implementation and evaluation," in *Proc. ACM WinTECH*, 2006, pp. 41–48.

¹⁰For example, in IEEE 802.11 standard [39], before association with an AP, there is a method for the AP to let stations that want to associate know the number of stations that are currently associated to itself. The number of associated stations is defined in the BSS Load element that can be delivered via either beacon or probe response frame. This way it is possible for stations to infer the number of active flows within a service coverage.

- [16] Y. Grunenberger, M. Heusse, F. Rousseau, and A. Duda, "Experience with an implementation of the idle sense wireless access method," in *Proc. ACM CoNEXT*, 2007, Art. no. 24.
- [17] Y. Kim, S. Choi, K. Jang, and H. Hwang, "Throughput enhancement of IEEE 802.11 WLAN via frame aggregation," in *Proc. IEEE VTC-Fall*, 2004, pp. 3030–3034.
- [18] W. Kim, H. K. Wright, and S. M. Nettles, "Improving the performance of multi-hop wireless networks using frame aggregation and broadcast for TCP ACKs," in *Proc. ACM CoNEXT*, 2008, Art. no. 27.
- [19] S. Sen, R. R. Choudhury, and S. Nelakuditi, "CSMA/CN: Carrier sense multiple access with collision notification," in *Proc. ACM MobiCom*, 2010, pp. 25–36.
- [20] T. Li *et al.*, "CRMA: Collision-resistant multiple access," in *Proc. ACM MobiCom*, 2011, pp. 61–72.
- [21] H. Jand, S.-Y. Yu, J. Shin, and Y. Yi, "Distributed learning for utility maximization over CSMA-based wireless multihop networks," in *Proc. IEEE INFOCOM*, 2014, pp. 280–288.
- [22] S.-Y. Yun, J. Shin, and Y. Yi, "CSMA over time-varying channels: Optimality, uniqueness and limited backoff rate," in *Proc. ACM Mobihoc*, 2013, pp. 137–146.
- [23] S.-Y. Yun, Y. Yi, J. Shin, and D. Y. Eun, "Optimal CSMA: A survey," in *Proc. ICCS*, 2012, pp. 199–204.
- [24] J. Lee *et al.*, "Implementing utility-optimal CSMA," in *Proc. Allerton Conf.*, 2009, pp. 102–111.
- [25] B. Nardelli *et al.*, "Experimental evaluation of optimal CSMA," in *Proc. IEEE INFOCOM*, 2011, pp. 1188–1196.
- [26] A. Aziz, D. Starobinski, P. Thiran, and A. Fawal, "EZ-Flow: Removing turbulence in IEEE 802.11 wireless mesh networks without message passing," in *Proc. ACM CoNEXT*, 2009, pp. 73–84.
- [27] R. Laufer, T. Salonidis, H. Lundgren, and P. L. Guyader, "XPRESS: A cross-layer backpressure architecture for wireless multi-hop networks," in *Proc. ACM MobiCom*, 2011, pp. 49–60.
- [28] A. Sharma and E. M. Belding, "FreeMAC: Framework for multi-channel mac development on 802.11 hardware," in *Proc. ACM PRESTO*, 2008, pp. 69–74.
- [29] H. Wu, Y. Peng, K. Long, S. Cheng, and J. Ma, "Performance of reliable transport protocol over IEEE 802.11 wireless LAN: Analysis and enhancement," in *Proc. IEEE INFOCOM*, 2002, pp. 599–607.
- [30] J. C. Bicket, "Bit-rate selection in wireless networks," Master's thesis, MIT, Cambridge, MA, USA, 2005.
- [31] G. Tan and J. Guttg, "Time-based fairness improves performance in multi-rate wireless LANs," in *Proc. USENIX*, 2004, pp. 269–282.
- [32] A. Proutiere, Y. Yi, T. Lan, and M. Chiang, "Resource allocation over network dynamics without timescale separation," in *Proc. IEEE INFOCOM*, 2010, pp. 1–5.
- [33] Y. Yi and M. Chiang, "chapter 9: Stochastic network utility maximization and wireless scheduling," in *Next-Generation Internet Architectures and Protocols*. Cambridge, U.K.: Cambridge University Press, 2011.
- [34] "Multiband Atheros driver for WiFi," 2014 [Online]. Available: <http://madwifi-project.org/>
- [35] "Optimal csma source code," 2015 [Online]. Available: <http://lanada.kaist.ac.kr/ocsma/>
- [36] L. Jiang and J. Walrand, "Approaching throughput-optimality in distributed csma scheduling algorithms with collisions," *IEEE/ACM Trans. Netw.*, vol. 19, no. 3, pp. 816–829, Jun. 2011.
- [37] "The Technology for all Wireless Project," 2015 [Online]. Available: <http://tfa.rice.edu/coverage.html>
- [38] M. J. Neely, "Super-fast delay tradeoffs for utility optimal fair scheduling in wireless networks," in *Proc. IEEE INFOCOM*, 2006, pp. 1–13.
- [39] *Wireless LAN Medium Access Control (MAC) and Physical Layer (PHY) Specifications*, IEEE Std 802.11-2012, Mar. 2012.



Jinsung Lee received the B.S. and Ph.D. degrees in electrical engineering from Korea Advanced Institute of Science and Technology (KAIST), Daejeon, Korea, in 2003 and 2012, respectively.

Since 2012, he has been with the DMC R&D Center, Samsung Electronics, Suwon, Korea. His research interests include the network architecture and protocol design for next-generation cellular systems and cross-layer optimization of multihop wireless networks.

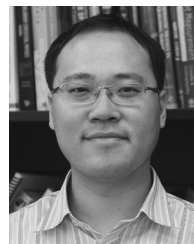
Dr. Lee was the recipient of the IEEE SECON Best

Paper Award in 2013.



Hojin Lee received the B.S. and Ph.D. degree in computer science and engineering from Seoul National University, Seoul, Korea, in 2003 and 2012, respectively.

He is a Senior Researcher with the Software R&D Center, Samsung Electronics, Suwon, Korea. Before joining Samsung Electronics, he was with Korea Advanced Institute of Science and Technology (KAIST), Daejeon, Korea, as a Postdoctoral Researcher from 2012 to 2014. He was a Visiting Researcher with the University of Minnesota, Minneapolis, MN, USA, in 2009, and with Simon Fraser University, Burnaby, BC, Canada, in 2005. His recent research interest includes neighbor discovery in Internet-of-Things (IoT) and realistic interference generation in wireless networks.



Yung Yi (S'04–M'06) received the B.S. and M.S. degrees in computer science and engineering from Seoul National University, Seoul, Korea, in 1997 and 1999, respectively, and the Ph.D. degree in electrical and computer engineering from the University of Texas at Austin, Austin, TX, USA, in 2006.

From 2006 to 2008, he was a Post-Doctoral Research Associate with the Department of Electrical Engineering, Princeton University, Princeton, NJ, USA. Now, he is an Associate Professor with the Department of Electrical Engineering, Korea Advanced Institute of Science and Technology (KAIST), Daejeon, Korea. His current research interests include the design and analysis of computer networking and wireless communication systems, especially congestion control, scheduling, and interference management, with applications in wireless ad hoc networks, broadband access networks, economic aspects of communication networks (a.k.a. network economics), and green networking systems.

Dr. Yi is now an Associate Editor of the IEEE/ACM TRANSACTIONS ON NETWORKING, *Journal of Communication Networks*, and *Computer Communications*. He was the recipient of two best paper awards at IEEE SECON 2013 and ACM Mobihoc 2013.



Song Chong (S'93–M'95) received the B.S. and M.S. degrees from Seoul National University, Seoul, Korea, in 1988 and 1990, respectively, and the Ph.D. degree from the University of Texas at Austin, Austin, TX, USA, in 1995, all in electrical engineering.

He is a Professor with the Department of Electrical Engineering, Korea Advanced Institute of Science and Technology (KAIST), Daejeon, Korea, and was the Head of Communication and Computing Division of the department in 2009 to 2010. He is the Founding Director of KAIST-LGE 5G Mobile Communications and Networking Research Center funded by LG Electronics. Prior to joining KAIST in 2000, he was with the Performance Analysis Department, AT&T Bell Laboratories, Holmdel, NJ, USA, as a Member of Technical Staff. His current research interests include wireless networks, mobile networks and systems, network data analytics, distributed algorithms, and cross-layer control and optimization.

Prof. Chong is currently an Editor of the IEEE/ACM TRANSACTIONS ON NETWORKING, IEEE TRANSACTIONS ON MOBILE COMPUTING, and IEEE TRANSACTIONS ON WIRELESS COMMUNICATIONS. He is the Technical Program Committee Co-Chair of IEEE SECON 2015 and has served on the Technical Program Committee of a number of leading international conferences including IEEE INFOCOM, ACM MobiCom, ACM CoNEXT, ACM Mobihoc, and IEEE ICNP. He serves on the Steering Committee of IEEE WiOpt and was the General Chair of IEEE WiOpt 2009. He received the IEEE William R. Bennett Prize in 2013 and the IEEE SECON Best Paper Award in 2013.



Edward W. Knightly (S'91–M'96–SM'04–F'09) received the B.S. degree from Auburn University, Auburn, AL, USA, in 1991, and the M.S. and Ph.D. degrees from the University of California, Berkeley, CA, USA, in 1992 and 1996, respectively, all in electrical engineering.

He is a Professor and the Department Chair of Electrical and Computer Engineering with Rice University, Houston, TX, USA. He leads the Rice Networks Group. The groups current projects include deployment, operation, and management of a

large-scale urban wireless network in a Houston under-resourced community. This network, Technology For All (TFA) Wireless, is serving over 4000 users in several square kilometers and employs custom-built programmable and observable access points. The network is the first to provide residential access in frequencies spanning from unused UHF TV bands to legacy WiFi bands (500 MHz–5 GHz). His group developed the first multiuser beamforming WLAN system that demonstrates a key performance feature provided by IEEE 802.11ac. His group also co-developed a clean-slate-design hardware platform for high-performance wireless networks, TAPs, and WARP. His research interests are in the areas of mobile and wireless networks with a focus on protocol design, performance evaluation, and at-scale field trials.

Prof. Knightly is a Sloan Fellow. He serves as an Editor-at-Large for the IEEE/ACM TRANSACTIONS ON NETWORKING and serves on the IMDEA Networks Scientific Council. He has chaired ACM MobiHoc, ACM MobiSys, IEEE INFOCOM, and IEEE SECON. He is a recipient of the National Science Foundation CAREER Award. He received Best Paper awards from ACM MobiCom, IEEE SECON, and the IEEE Workshop on Cognitive Radio Architectures for Broadband.



Mung Chiang (S'00–M'03–SM'08–F'12) received the B.S. (Hons.) degree in electrical engineering and mathematics and the M.S. and Ph.D. degrees in electrical engineering from Stanford University, Stanford, CA, USA, in 1999, 2000, and 2003, respectively.

He is the Arthur LeGrand Doty Professor of Electrical Engineering with Princeton University, Princeton, NJ, USA. A 2007 Technology Review TR35 Young Innovator, he created the Princeton EDGE Lab in 2009 to bridge the theory-practice divide in networking by spanning from proofs to prototypes, resulting in a few technology transfers to industry and several startup companies. He is Chairman of the Princeton Entrepreneurship Advisory Committee and Director of the Keller Center for Innovations in Engineering Education, and was selected as a 2014 New Jersey (non-profit) CEO of the Year by the NJ Technology Council. His massive open online courses on networks have reached about 250 000 students since 2012. His research has been on network utility maximization and network function allocation, fog networks and IoT, smart data pricing, and social learning networks.

Prof. Chiang was named a Guggenheim Fellow in 2014. He received the 2013 Alan T. Waterman Award and the 2012 IEEE Kiyo Tomiyasu Award. He coauthored papers that received the IEEE INFOCOM 2012 Best Paper Award and the IEEE SECON 2013 Best Paper Award and led to a Yelp Data Challenge 2014 Grand Prize. He received the 2013 Terman Award from the American Society of Engineering Education, and the textbook *Networked Life: 20 Questions and Answers* received the 2012 PROSE Award in Science and Engineering by the Association of American Publishers.